

Asymptotic state observers for a simplified brass instrument model

Brigitte d'Andréa-Novel^{*†}

*Mines ParisTech - Centre de Robotique,
60 boulevard Saint-Michel, 75272 Paris Cedex 06, France*

Jean-Michel Coron[‡]

*Université Pierre et Marie Curie - Laboratoire Jacques-Louis Lions,
Institut Universitaire de France,
B.C. 196,
4 place Jussieu
75252 Paris Cedex 05, France*

Thomas Hélie^{§¶}

*IRCAM - CNRS UMR 9912 Sciences et Technologies de la Musique et du Son,
1 place Igor Stravinsky,
75004 Paris, France*

(Dated: 7th January 2010)

* Note that the co-authors are listed with respect to the alphabetical order.

§ Corresponding Author

Abstract

In this paper, a simplified model of a brass instrument is introduced. It is composed of a valve (including the mechanics of the lips), a jet (coupled with the valve dynamics), and a straight acoustic pipe excited by the jet, radiating in the air, and with frequency independent losses. This model couples an ordinary differential equation (valve) to a partial differential equation (acoustic pipe) through a static nonlinear function (Bernoulli relation on the jet). In fact, the overall system can be described by a “so-called” nonlinear neutral state space representation, the state of which being the position and velocity of the valve aperture and the ingoing wave of pressure at the entrance of the pipe. The measured output is the pressure at the open end of the pipe and the control is the mouth pressure. In this paper, methods of control engineering are applied to recover the state from the input and the measured output, assuming that propagation characteristics and player expression parameters are constant: a nonlinear state observer is built. The robustness to wrong initial conditions and to noise on the measured output are analyzed.

PACS numbers: 60.014, 75.005, 75.020

[†]Electronic address: brigitte.dandrea-novel@mines-paristech.fr

[‡]Electronic address: coron@ann.jussieu.fr

[¶]Electronic address: thomas.helie@ircam.fr

I. INTRODUCTION

Many physical models of musical instruments are available in the literature [1, 2]. But their control to obtain realistic musical restitution is usually a problem, especially for self-sustained instruments. Inversion of the model therefore appears as a natural tool to cope with this problem, i.e., recovering the control parameters from a target sound. This problem has already been investigated in the past [3, 4] using control engineering techniques, but significant improvements are still needed.

A problem to cope with consists in recovering both the vibro-acoustic state and the musician’s control parameters from a unique observation, namely, the sound produced. The difficulty is increased by the fact that self-sustained instruments are able to generate a large variety of regimes and, possibly, complex regimes such as chaotic ones [5]. Nevertheless, what can be noticed for these systems is the fact that two separate time-scales can be considered. Vibrating variables x (such as acoustic pressure, reed or lips motion, etc) oscillate mainly at high frequencies compared to the control variables associated with the player’s gestures G (pressure in the mouth, lip stiffness, etc).

Then, assuming some usual quantities are measured on the system, such as the pressure radiated at the end of the instrument, called the “output” y , the inversion could be performed in two steps :

- (P1) [the first step consists in recovering the full oscillating internal state \$x\$ of the instrument from the knowledge of \$y\$, assuming the control \$G\$ is locally constant](#) . This is achieved by building a so-called “state observer” in control systems theory [6, 7];
- (P2) the second one consists in computing the accessible parameters G from this observed state. This could be achieved using adaptive filtering techniques [8, 9].

This paper addresses the first problem (P1) of elaborating a state observer for a simplified brass instrument model, assuming that the output y is the pressure at the end of the pipe. [The observer is elaborated from the nonlinear neutral state space representation associated to the overall system, using Lyapunov techniques. Other approaches based on e.g. sliding modes can be found in \[10\].](#)

The structure of the paper is as follows : section II introduces a simplified physical description of the instrument. Section III proposes a state-space representation of the in-

strument deduced from the model of section II. Section IV is dedicated to the elaboration of the state observer. Section V presents some simulation results. Conclusion and perspectives will be presented in section VI.

II. DESCRIPTION OF THE INSTRUMENT AND PHYSICAL EQUATIONS

Consider a simplified instrument, of the brass instrument type, composed of (see Fig.1),

- *a valve*, the aperture of which is modulated by a [single](#) solid characterized by its mass, stiffness and damping,
- *a jet* which applies a force on the valve,
- *an acoustic pipe* the vibrations of which are set in motion by the jet.

Each component is modeled as detailed below.

Moreover, the absolute pressure is denoted by the capital letter P and the relative pressure by $p = P - P_{atm}$ where P_{atm} is the atmospheric pressure. In the mouth, the (relative) pressure is denoted p_m and the particle velocity v_m . They are respectively denoted p_{jet} and v_{jet} in the jet.

A. Valve

The lips of the musician are represented by a one degree of freedom lip model: a valve composed of a trapezoid-parallelepipedic solid \mathcal{S} with mass m , moving in the vertical direction, subjected to pressure forces F_{side} and F_{bot} , a damping a , and a spring with stiffness k . The bottom of the mass is located by the variable $\xi(t)$ and an open valve corresponds to $\xi > 0$. The equilibrium position at rest is denoted by $\xi(t) = \xi_e$ which is supposed to be positive.

The dynamics of the solid \mathcal{S} are governed by

$$m\ddot{\xi} + a\dot{\xi} + k(\xi - \xi_e) = F_{side} + F_{bot}. \quad (1)$$

The vertical component of the force due to the pressure on the sides of \mathcal{S} is

$$F_{side} = (A_{side} \sin \theta) (p_m - p_0), \quad (2)$$

where the area A_{side} of the lateral sides of \mathcal{S} and the angle θ in Fig.1 are supposed to be constant. The force F_{bot} applied on the bottom side of \mathcal{S} depends on the sign of ξ :

- If the valve is open, F_{bot} is due to the jet pressure p_{jet} so that

$$\text{if } \xi > 0, \quad F_{bot} = A_{bot} p_{jet}, \quad (3)$$

- If the valve is closed, F_{bot} is a contact force. An empirical model of a contact with a second lip (rather than with a non-realistic rigid body) is given by [11]

$$\text{if } \xi \leq 0, \quad F_{bot} = -m\kappa_m \ddot{\xi} - a\kappa_a \dot{\xi} - k\kappa_k (\xi - \xi_e). \quad (4)$$

Coefficients κ_m , κ_a , and κ_k respectively correspond to an additional mass, damping and stiffness due to the contact of the two lips. Some empirical values of these corrections are $(\kappa_m, \kappa_a, \kappa_k) = (1, 4, 3)$ [12–14].

The equilibrium position ξ_e is a constant parameter set by the musician such that (1) is satisfied ($\xi = \xi_e$) with $p_m = p_{jet} = p_0 = 0$ and (arbitrary) constants m , a , k . Moreover, the mouth pressure p_m and parameters $(m, a, k, \kappa_m, \kappa_a, \kappa_k, A_{side}, A_{bot})$ are characteristic of the musician.

Note that more refined models of the lips mechanics have been studied: a two-dimensional lip vibration model used for the trumpet sound synthesis can be found in e.g. [15].

B. Aperture geometry and jet

If $\xi \leq 0$, the valve is closed and there is no jet. If $\xi > 0$, there is a jet under the solid \mathcal{S} . The geometry of the aperture is supposed to be rectangular with an area

$$A(t) = \ell \xi(t), \quad (5)$$

(ℓ is the lip width) much smaller than that of the mouth section A_m so that $A \ll A_m$. The jet is considered to be governed by the Bernoulli equation (quasi-steady jet and losses ignored)

$$p_m + \frac{1}{2}\rho v_m^2 = \frac{1}{2}\rho v_{jet}^2 + p_{jet}. \quad (6)$$

From the conservation of the airflow, the particle speed $|v_m| = |\frac{A}{A_m}v_{jet}| \ll |v_{jet}|$ is neglected in (6). Finally, for relative pressures, this yields

$$p_m = \frac{1}{2}\rho v_{jet}^2 + p_{jet}, \text{ if } \xi > 0, \quad (7)$$

$$v_{jet} = 0, \text{ if } \xi \leq 0. \quad (8)$$

Remark 1 From (7), $p_m \geq p_{jet}$ so that the jet is oriented from the mouth towards the pipe, that is,

$$v_{jet} \geq 0.$$

More elaborate models which authorize negative v_{jet} have also been proposed [16]. This case will not be considered in the present paper.

C. Acoustic pipe and boundary conditions

Consider the linear acoustic propagation of plane waves in a lossless straight pipe with section S and length L . It is described by the conservative equations

$$\partial_t \begin{bmatrix} p \\ u \end{bmatrix} + \begin{bmatrix} 0 & \frac{\rho c^2}{S} \\ \frac{S}{\rho} & 0 \end{bmatrix} \partial_z \begin{bmatrix} p \\ u \end{bmatrix} = \begin{bmatrix} 0 \\ 0 \end{bmatrix} \quad \forall z \in [0, L], \quad (9)$$

where $p(z, t)$ is the pressure at location z and at time t in the pipe, u is the airflow and c is the celerity of the wave. Using the change of functions

$$\begin{bmatrix} p^+ \\ p^- \end{bmatrix} = M \begin{bmatrix} p \\ u \end{bmatrix} \quad (10)$$

where $M = \frac{1}{2} \begin{bmatrix} 1 & Z_c \\ 1 & -Z_c \end{bmatrix}$, $M^{-1} = \begin{bmatrix} 1 & 1 \\ 1/Z_c & -1/Z_c \end{bmatrix}$ and $Z_c = \rho c/S$ is the characteristic impedance, the conservative equations yield

$$\partial_t p^+ + c \partial_z p^+ = 0, \quad (11)$$

$$\partial_t p^- - c \partial_z p^- = 0, \quad (12)$$

which govern decoupled progressive waves and solve into

$$p^\pm(z, t) = p_0^\pm(t \mp z/c). \quad (13)$$

The boundary conditions are the following:

- at $z = 0$ (connection between the jet and the acoustic pipe), the airflow and pressure are assumed to be continuous, following remarks of Hirschberg [17] (experimental validations has been also obtained for the mouthpiece of a clarinet [18]):

$$p_{jet}(t) = p(0, t) = p_0^+(t) + p_0^-(t), \quad (14)$$

$$A(t) v_{jet} = u_{jet}(t) = u(0, t) = \frac{p_0^+(t) - p_0^-(t)}{Z_c}. \quad (15)$$

- at $z = L$, consider the non homogeneous boundary condition given by $p(z = L, t) = Z_L u(z = L, t)$ with a real passive impedance $Z_L > 0$. From (9) and (13), this expression translates into

$$p_0^-(t) = \lambda p_0^+(t - \tau), \quad (16)$$

$$\tau = 2L/c, \quad (17)$$

$$\lambda = (Z_L - Z_c)/(Z_L + Z_c) \in (-1, 1). \quad (18)$$

Notice that this boundary condition is very simplified compared to realistic radiation impedances. But it allows to catch basic versions of the main effects. For instance, the usual correction of the pipe length due to the imaginary part of the radiation impedance can be included in the length L (simplified case of a constant length correction). Moreover, the radiated energy which is lost by an open pipe involves a small real positive impedance part. Here, $Z_L \ll Z_c$ (so that $\lambda < 0$) models a frequency-independent version of such a phenomenon.

In the discussion which follows, the notation $p^\pm(t)$ will be used rather than $p_0^\pm(t)$.

III. STATE-SPACE REPRESENTATION

A. Definitions of neutral systems, state, input, output, and reduced parameters

A neutral system [19, 20] is a delay differential system with the general expression

$$\dot{x}(t) = f(x(t), x(t - \tau), \dot{x}(t - \tau), w(t)) \quad (19)$$

$$y(t) = g(x(t), x(t - \tau), \dot{x}(t - \tau), w(t)) \quad (20)$$

where the function f is responsible for the dynamics of the system and g defines the measured quantity. As detailed below, the model presented in section II can be represented by such a system, where the state $x = [x_1, x_2, x_3]^T$, the input $w = [w_1, w_2]^T$, and the output y are defined by

$$x(t) = [\xi(t) - \xi_e, \dot{\xi}(t), p^+(t)]^T, \quad (21)$$

$$w(t) = [p_m(t), \dot{p}_m(t)]^T, \quad (22)$$

$$y(t) = (1 + \lambda) p^+(t - \tau/2). \quad (23)$$

Note that $y(t) = p(L, t)$ is the pressure measured at the output of the pipe **and that the time derivative \dot{p}_m of the mouth pressure will be necessary when establishing the neutral state-space representation (see section III C).**

In this paper, the instrument is considered to be at rest before $t = 0$ so that x , w , and y are zero for $t < 0$. Moreover, quantities ξ_e , m , a , k , A_{side} , A_{bot} , θ , ρ , c , S , L , ℓ , λ , κ_m , κ_a , κ_k introduced in section II are all supposed to be constant. It will appear that the neutral system depends on the reduced constant parameters $\Theta = [\alpha^\pm, \omega^\pm, \beta_0^\pm, \beta_m^\pm, \lambda, \mu, \tau]$ defined in table I. The equations of the neutral system for the brass instrument are derived below.

B. Mechanics of the lips

Combining equations (1) to (4) and (16) yields the following equations:

$$\begin{aligned} \text{if } \xi > 0, \quad \ddot{\xi}(t) + \alpha^+ \dot{\xi}(t) + (\omega^+)^2 (\xi(t) - \xi_e) = \\ \beta_0^+ (p^+(t) + \lambda p^+(t - \tau)) + \beta_m^+ p_m(t), \end{aligned} \quad (24)$$

$$\begin{aligned} \text{if } \xi \leq 0, \quad \ddot{\xi}(t) + \alpha^- \dot{\xi}(t) + (\omega^-)^2 (\xi(t) - \xi_e) = \\ \beta_0^- (p^+(t) + \lambda p^+(t - \tau)) + \beta_m^- p_m(t), \end{aligned} \quad (25)$$

where the coefficients are given in Tab.I. Hence, from (21), (23), it follows that, writing $\sigma = \text{sign}(\xi)$,

$$\dot{x}_1(t) = x_2(t), \quad (26)$$

$$\begin{aligned} \dot{x}_2(t) = -(\omega^\sigma)^2 x_1(t) - \alpha^\sigma x_2(t) \\ + \beta_0^\sigma (x_3(t) + \lambda x_3(t - \tau)) + \beta_m^\sigma w_1(t). \end{aligned} \quad (27)$$

C. Jet and acoustics

1. Case $\xi > 0$

Using (5) and (14-16), equations (7) rewrite as follows:

$$p_m(t) = \frac{\mu}{2} \left(\frac{p^+(t) - \lambda p^+(t - \tau)}{\xi(t)} \right)^2 + p^+(t) + \lambda p^+(t - \tau), \quad (28)$$

where the coefficients are given in Tab. I. Then, writing

$$D(t) = 1 + \mu \frac{p^+(t) - \lambda p^+(t - \tau)}{(\xi(t))^2}, \quad (29)$$

and isolating $\dot{p}^+(t)$ from the time derivative of (28) yields

$$\begin{aligned} \dot{p}^+(t) &= \frac{\dot{p}_m(t) - 2\lambda\dot{p}^+(t - \tau) + \mu \frac{\dot{\xi}(t)(p^+(t) - \lambda p^+(t - \tau))^2}{\xi(t)^3}}{D(t)} \\ &\quad + \lambda\dot{p}^+(t - \tau). \end{aligned}$$

Then, using (28) to substitute for $\left(\frac{p^+(t) - \lambda p^+(t - \tau)}{\xi(t)} \right)^2$ in the above equation leads to

$$\begin{aligned} \dot{p}^+(t) &= \frac{\dot{p}_m(t) - 2\lambda\dot{p}^+(t - \tau) + \frac{2\dot{\xi}(t)(p_m(t) - p^+(t) - \lambda p^+(t - \tau))}{\xi(t)}}{D(t)} \\ &\quad + \lambda\dot{p}^+(t - \tau). \end{aligned} \quad (30)$$

Remark 2 For initial condition of (p_m, p^+, ξ) satisfying (28) at $t = 0$, the trajectory of (30) also satisfies (28) for $t > 0$. Equation (30) is then weaker than (28) but will be useful to derive the expected neutral state-space representation.

Remark 3 For closing lips, that is $\xi(t) \rightarrow 0^+$, the behavior of p^+ is such that, from (28),

$$p^+(t) \underset{0^+}{=} \lambda p^+(t - \tau) + \xi(t) \sqrt{\frac{2}{\mu}(p_m(t) - 2\lambda p^+(t - \tau))} + \mathcal{O}(\xi^2(t))$$

so that, in (29), excluding the case $p_m(t) = 2\lambda p^+(t - \tau)$,

$$\frac{(\xi(t))^2}{p^+(t) - \lambda p^+(t - \tau)} \underset{0^+}{=} \frac{\xi(t)}{\sqrt{\frac{2}{\mu}(p_m(t) - 2\lambda p^+(t - \tau))}} + \mathcal{O}(\xi^2(t)),$$

and, in (30),

$$\dot{p}^+(t) \underset{0^+}{=} \lambda\dot{p}^+(t - \tau) + \sqrt{2\mu(p_m(t) - 2\lambda p^+(t - \tau))}\dot{\xi}(t) + \mathcal{O}(\xi(t)).$$

2. Case $\xi \leq 0$

Similarly, equation (8) and the time derivative of its left and right hand sides rewrite as follows:

$$p^+(t) = \lambda p^+(t - \tau), \quad (31)$$

$$\dot{p}^+(t) = \lambda \dot{p}^+(t - \tau). \quad (32)$$

3. General expression

Equations (30,32) are summarized by the following unique equation :

$$\dot{x}_3(t) = \frac{\sigma+1}{2} \left[\frac{w_2(t) - 2\lambda \dot{x}_3(t-\tau) + \frac{2x_2(t)(w_1(t) - x_3(t) - \lambda x_3(t-\tau))}{x_1(t) + \xi_e}}{1 + \mu \frac{x_3(t) - \lambda x_3(t-\tau)}{(x_1(t) + \xi_e)^2}} \right] + \lambda \dot{x}_3(t - \tau). \quad (33)$$

D. Final neutral state-space representation

Equations (21-23) and (26,27,33) define the model of the instrument as a *nonlinear neutral system*, that is, a system described by (19-20). More precisely, functions f and g have the simple formulations

$$f(x(t), x(t-\tau), \dot{x}(t-\tau), w(t)) = F(x(t), x_3(t-\tau), \dot{x}_3(t-\tau), w(t)) \quad (34)$$

$$g(x(t), x(t-\tau), \dot{x}(t-\tau), w(t)) = C x(t - \tau/2), \quad (35)$$

where C is the observation matrix $C = [0, 0, 1 + \lambda]$ and F is given by, for all **the formal variables** $(X, Y, Z, W) \in \mathbb{R}^3 \times \mathbb{R} \times \mathbb{R} \times \mathbb{R}^2$,

$$F_1(X, Y, Z, W) = [0, 1, 0]X, \quad (36)$$

$$F_2(X, Y, Z, W) = -(\omega^\sigma)^2 X_1 - \alpha^\sigma X_2 + \beta_0^\sigma X_3 \\ + \lambda \beta_0^\sigma Y + \beta_m^\sigma W_1, \quad (37)$$

$$F_3(X, Y, Z, W) = \frac{W_2 - 2\lambda Z + \frac{2X_2(W_1 - X_3 - \lambda Y)}{X_1 + \xi_e}}{1 + \mu \frac{X_3 - \lambda Y}{(X_1 + \xi_e)^2}} \\ + \lambda Z, \quad \text{if } X_1 + \xi_e > 0, \quad (38)$$

$$F_3(X, Y, Z, W) = \lambda Z, \quad \text{if } X_1 + \xi_e \leq 0, \quad (39)$$

recalling that, in (37), σ denotes symbol $+$ if $\xi = X_1 + \xi_e > 0$ and symbol $-$ otherwise. Expressions (36-37,39) are linear with respect to X, Y, Z, W while (38) is the nonlinearity responsible for the self-oscillation of the musical instrument.

Remark 4 *The difficulties due to the discontinuities in (37-39) when $\text{sign}(\xi)$ changes, are not examined here. Nevertheless, numerical results presented in section V show that the case $\xi < 0$ is sparse and that deriving the observer with no special treatment of these discontinuities (section IV) yet produces a quite satisfying behaviour.*

In order to obtain a non delayed version of the output, the following change of state is introduced

$$\tilde{x}(t) = x(t - \tau/2),$$

so that (19) and (20) rewrite

$$\dot{\tilde{x}}(t) = F(\tilde{x}(t), \tilde{x}_3(t - \tau), \dot{\tilde{x}}_3(t - \tau), w(t - \tau/2)), \quad (40)$$

$$y(t) = C \tilde{x} = \tilde{x}_3(t). \quad (41)$$

For sake of simplicity, we will keep in (40-41) the notation $x(t)$ in place of $\tilde{x}(t)$.

Remark 5 *Following remark 2, the neutral system given by (36-41) describes the physical model of our instrument if the initial conditions satisfy (28) or (31), namely, at $t = 0$,*

$$W_1 = \frac{\mu}{2} \left(\frac{X_3 - \lambda Y}{X_1 + \xi_e} \right)^2 + X_3 + \lambda Y, \quad \text{if } X_1 + \xi_e > 0, \\ X_3 = \lambda Y, \quad \text{otherwise.}$$

IV. STATE-OBSERVER

As mentioned in the introduction, the problem which is considered here is the construction of an asymptotic state observer, assuming that the constant parameters Θ and the mouth pressure p_m are known. The idea is to use an extended Kalman filter type observer [21] elaborated from the nonlinear neutral system presented in section III. This observer will depend on the output error but also on its delayed value.

The gain matrices of the observer will be chosen to stabilize the linear time-varying neutral system governing the linearized equation of the estimation error vector. The proof of stability relies on a suitable Lyapunov function. The links with the local stability of the nonlinear error equation will be discussed.

A. Definition of the observer

The following state observer for system (40-41) is proposed :

$$\begin{aligned} \dot{\hat{x}}(t) = & F(\hat{x}(t), \hat{x}_3(t-\tau), \dot{\hat{x}}_3(t-\tau), w(t-\tau/2)) \\ & - \Lambda_1(y(t) - \hat{y}(t)) - \Lambda_2(y(t-\tau) - \hat{y}(t-\tau)), \end{aligned} \quad (42)$$

where Λ_1 and Λ_2 are 3×1 gain matrices.

B. Linearized error equation

Let e denote the estimation error vector:

$$e = x - \hat{x}. \quad (43)$$

The matrices Λ_1 and Λ_2 will be chosen such that the following linearized dynamical equation of the estimation error is locally asymptotically stable :

$$\dot{e}(t) = \widehat{\mathbb{A}}(t) e(t) + \widehat{\mathbb{B}}(t) e_3(t-\tau) + \widehat{\mathbb{H}}(t) \dot{e}_3(t-\tau), \quad (44)$$

where

$$\mathbb{A}(X, Y, Z, W) = \frac{\partial F}{\partial X}(X, Y, Z, W) + \Lambda_1 C, \quad (45)$$

$$\mathbb{B}(X, Y, Z, W) = \frac{\partial F}{\partial Y}(X, Y, Z, W) + \Lambda_2 [C]_3, \quad (46)$$

$$\mathbb{H}(X, Y, Z, W) = \frac{\partial F}{\partial Z}(X, Y, Z, W). \quad (47)$$

and $\widehat{\mathbb{A}}(t) = \mathbb{A}(\hat{x}(t), \hat{x}_3(t - \tau), \dot{\hat{x}}_3(t - \tau), w(t))$ and similarly for $\widehat{\mathbb{B}}(t)$ and $\widehat{\mathbb{H}}(t)$.

This property will be proved in Theorem 1, section IV D, the proof of which relies on the following technical lemmas.

Remark 6 *In the case of lips (versus to the case of reeds), θ is positive (see Fig. 1). Moreover, for closed lips the energy in the pipe is dissipated by the real passive impedance modeling the radiation (see (16)). Then, playing the musical instrument in a standard way (blowing situation, $p_m > 0$) involves that the lips cannot be blocked in a closed configuration. Moreover, the empirical values $(\kappa_m, \kappa_a, \kappa_k) = (1, 4, 3)$ used for the contact force (see (4)) help the system leave a “closed lips” configuration faster than with no contact force. In practice, the system mainly operates with open lips.*

C. Technical lemmas

Lemma 1 *The gain matrix Λ_2 can be chosen such that $\widehat{\mathbb{B}}(t)$ in equation (44) is zero.*

Proof : From (36-39) and denoting $\Lambda_2 = [\lambda_{21}, \lambda_{22}, \lambda_{23}]^T$, it can be easily shown that:

$$\mathbb{B}(X, Y, Z, W) = \begin{pmatrix} (1+\lambda)\lambda_{21} \\ \beta_1^\sigma + (1+\lambda)\lambda_{22} \\ \frac{\partial F_3}{\partial Y} + (1+\lambda)\lambda_{23} \end{pmatrix}$$

where it is then clear that the λ_{2i} , $i = 1, \dots, 3$ can be chosen such that $\widehat{\mathbb{B}}$ is the null matrix. This ends the proof. \diamond

Remark 7 *From lemma 1, the gain matrix Λ_2 in the observer equation (42) will be time dependent and a function of $X = \hat{x}(t)$, $Y = \hat{x}_3(t - \tau)$, $Z = \dot{\hat{x}}_3(t - \tau)$, $W = w(t - \tau/2)$.*

Lemma 2 *The matrix $\mathbb{H}(t) = \mathbb{H}(x(t), x_3(t - \tau), \dot{x}_3(t - \tau), w(t - \tau/2))$ defined from (47) is such that :*

$$|\mathbb{H}(t)| \leq |\lambda| < 1.$$

Proof : First, if $X_3 - \lambda Y \geq 0$, then $|\mathbb{H}(X, Y, Z, W)| \leq |\lambda|$. Indeed, from (36-39), it follows

that $\mathbb{H}(X, Y, Z, W) = [0, 0, H_3(X, Y, Z, W)]^T$ with

$$\begin{aligned} H_3(X, Y, Z, W) &= \frac{\partial F_3(X, Y, Z, W)}{\partial Z} \\ &= \lambda \frac{1 - G(X, Y, Z)}{1 + G(X, Y, Z)}, \end{aligned} \quad (48)$$

where $G(X, Y, Z) = (X_1 + \xi_e)^2 / (\mu(X_3 - \lambda Y))$ if $X_1 + \xi_e > 0$ (see Remark 3) and $G(X, Y, Z) = 0$ otherwise. Now, $|1 - G(X, Y, Z)| / |1 + G(X, Y, Z)| \leq 1$ if and only if $G(X, Y, Z) \geq 0$. This last condition is satisfied if $X_3 - \lambda Y \geq 0$.

Second, from equations (7,8) and following Remark 1, $v_{jet}(t) \geq 0$. Then, from equations (15,16) and since $A(t) \geq 0$, it follows that $p^+(t) = \lambda p^+(t - \tau) + A(t) Z_c v_{jet}(t) \geq \lambda p^+(t - \tau)$. This concludes the proof, taking $X = x(t)$, $Y = x_3(t - \tau)$. \diamond

Remark 8 Since $|\lambda| < 1$, the inequality $|\widehat{\mathbb{H}}(t)| < 1$ will be also satisfied for a sufficiently small estimation error.

Lemma 3 Let $\chi > 0$. The matrix gain Λ_1 can be chosen such that $\widehat{\mathbb{A}}(t)$ in equation (44) takes the following form :

$$\widehat{\mathbb{A}} = \left(\begin{array}{cc|c} 0 & 1 & 0 \\ -(\omega^{\hat{\sigma}})^2 & -\alpha^{\hat{\sigma}} & 0 \\ \widehat{\mathbb{M}}_{31} & \widehat{\mathbb{M}}_{32} & -\chi \end{array} \right)$$

where $\hat{\sigma} = \text{sign}(\xi_e + \hat{x}_1)$ and $\widehat{\mathbb{M}}(t) = \mathbb{M}(\hat{x}(t), \hat{x}_3(t - \tau), \hat{x}_3(t - \tau), w(t - \tau/2))$ with $\widehat{\mathbb{M}} = \frac{\partial F}{\partial X}(X, Y, Z, W)$. This choice of Λ_1 ensures that e_1 and e_2 are decoupled from e_3 's dynamics.

Proof : From (36-39), and denoting $\Lambda_1 = [\lambda_{11}, \lambda_{12}, \lambda_{13}]^T$,

$$\widehat{\mathbb{A}} = \widehat{\mathbb{M}} + \Lambda_1 C = \widehat{\mathbb{M}} + (1 + \lambda) \begin{pmatrix} 0 & 0 & \lambda_{11} \\ 0 & 0 & \lambda_{12} \\ 0 & 0 & \lambda_{13} \end{pmatrix}.$$

Denote $F = \widehat{\mathbb{M}}_{1:2,1:2} = \begin{pmatrix} 0 & 1 \\ -(\omega^{\hat{\sigma}})^2 & -\alpha^{\hat{\sigma}} \end{pmatrix}$. The result is then obtained by choosing

$$\Lambda_1 = \frac{1}{1 + \lambda} \left(\begin{bmatrix} 0 \\ 0 \\ -\chi \end{bmatrix} - \widehat{\mathbb{M}} \begin{bmatrix} 0 \\ 0 \\ 1 \end{bmatrix} \right) = \begin{bmatrix} 0 \\ -\beta_0^{\hat{\sigma}} \\ -\chi - \widehat{\mathbb{M}}_{33} \end{bmatrix}$$

and noticing that $\bar{e} = [e_1, e_2]^T$ satisfies the following dynamical equation :

$$\dot{\bar{e}} = F\bar{e} \quad (49)$$

where the constant matrix F is Hurwitz. \diamond

Remark 9 *The matrix F is constant (with respect to the time) for open lips ($\sigma > 0$). The same holds for closed lips (see remark 6).*

D. Main stability result

The main stability result is stated by the following theorem.

Theorem 1 *There exist positive constants $\kappa > 0$ and $\eta > 0$, such that for every solution of equation (44), the following inequality holds :*

$$\begin{aligned} & \left(e_1^2(t) + e_2^2(t) + e_3^2(t) + \int_{t-\tau}^t \dot{e}_3^2(s) ds \right) \leq \\ & \kappa e^{-\eta t} \left(e_1^2(0) + e_2^2(0) + e_3^2(0) + \int_{-\tau}^0 \dot{e}_3^2(s) ds \right). \end{aligned} \quad (50)$$

Proof : From lemma 3, F being Hurwitz, define the symmetric positive definite matrix P solution of the matrix Lyapunov equation [7] :

$$F^T P + P F = -I_{2 \times 2}$$

$I_{2 \times 2}$ denoting the 2×2 identity matrix.

Now, consider the following Lyapunov function candidate where $C > 0$, $K > 0$ and $\nu > 0$ are suitable positive constants :

$$V = C \frac{e_3^2}{2} + K \bar{e}^T P \bar{e} + \int_{t-\tau}^t \dot{e}_3^2(s) e^{-\nu(t-s)} ds. \quad (51)$$

Let us recall the estimation error equation (44), that is,

$$\dot{e}(t) = \widehat{\mathbb{A}}(t) e(t) + \widehat{\mathbb{B}}(t) e_3(t - \tau) + \widehat{\mathbb{H}}(t) \dot{e}_3(t - \tau)$$

where $\widehat{\mathbb{A}}$ is given in lemma 3, $\widehat{\mathbb{B}}$ is zero using lemma 1 and $\widehat{\mathbb{H}} = [0, 0, \widehat{H}_3]^t$ is defined as in lemma 2.

If the constant C is chosen to be equal to $C = 2\chi$, where $\chi > 0$ is defined in lemma 3, the time derivative of V along the solutions of the dynamical equations of the [above observation error](#) can be written as follows :

$$\dot{V} = T_1 + T_2 + T_3 \quad (52)$$

where

$$\begin{aligned}
T_1 &= -\chi^2 e_3^2 - \dot{e}_3^2(t - \tau)(e^{-\nu\tau} - \hat{H}_3^2(t)) \\
&\quad - K(e_1^2 + e_2^2) \\
&\quad - \nu \int_{t-\tau}^t \dot{e}_3^2(s) e^{-\nu(t-s)} ds,
\end{aligned} \tag{53}$$

$$T_2 = (\hat{M}_{31}e_1 + \hat{M}_{32}e_2)^2, \tag{54}$$

$$T_3 = 2\hat{H}_3(\hat{M}_{31}e_1\dot{e}_3(t - \tau) + \hat{M}_{32}e_2\dot{e}_3(t - \tau)), \tag{55}$$

where \hat{M}_{31} and \hat{M}_{32} are defined in lemma 3.

Notice that for all $\epsilon > 0$ and for all e_1, e_2 and $e_3(t - \tau)$, the following inequalities hold for some positive constants R_1 and R_2 :

$$T_3 \leq \frac{1}{\epsilon}(e_1^2 + e_2^2) + R_1\epsilon\dot{e}_3^2(t - \tau) \tag{56}$$

and

$$T_2 \leq R_2(e_1^2 + e_2^2). \tag{57}$$

Moreover, from lemma 2, if the constant ν in V is chosen sufficiently small, $(e^{-\nu\tau} - \hat{H}_3^2(t)) \geq e^{-\nu\tau} - \lambda^2 \geq \delta > 0$, for all t and $\tau \in [0, 2L/c]$, so that :

$$\begin{aligned}
\dot{V} &\leq -\chi^2 e_3^2 - \delta\dot{e}_3^2(t - \tau) \\
&\quad - (K - R_2)(e_1^2 + e_2^2) \\
&\quad + \frac{1}{\epsilon}(e_1^2 + e_2^2) + R_1\epsilon\dot{e}_3^2(t - \tau) \\
&\quad - \nu \int_{t-\tau}^t \dot{e}_3^2(s) e^{-\nu(t-s)} ds.
\end{aligned} \tag{58}$$

Choose

$$\epsilon = \frac{\delta}{2R_1} \tag{59}$$

which leads to :

$$\begin{aligned}
\dot{V} &\leq -\chi^2 e_3^2 - \frac{\delta}{2}\dot{e}_3^2(t - \tau) \\
&\quad - (K - R_2 - \frac{2R_1}{\delta})(e_1^2 + e_2^2) \\
&\quad - \nu \int_{t-\tau}^t \dot{e}_3^2(s) e^{-\nu(t-s)} ds.
\end{aligned} \tag{60}$$

Then, for $K = R_2 + \frac{4R_1}{\delta}$ and for a suitable positive constant $\eta > 0$, the following inequality holds:

$$\dot{V} \leq -\eta V \tag{61}$$

which ends the proof. \diamond

Notice that the weight $e^{\pm\nu x}$ in the integral term of the Lyapunov function is essential to get a **strict** Lyapunov function. It is similar to the one introduced by Castelan and Infante [22] for matrix difference differential equations and also by Coron [23] to stabilize the Euler equation of incompressible fluids. More recently, it has also been used for linear symmetric hyperbolic systems [24] and for exponential stabilization of one-dimensional nonlinear hyperbolic systems [25, 26].

V. SIMULATION RESULTS AND DISCUSSION

Observation results have been performed on outputs y , simulated using an Euler explicit scheme on (40), that is, using the recursive equations $x((n+1)T) = x(nT) + T\delta x(nT)$ with $\delta x(nT) = T F\left(x(nT), x_3((n-2N)T), \delta x((n-2N)T), w(n-N)T\right)$ where T is the sampling period (T and the length L are chosen such that $N = \tau/(2T)$ is integer). To be more realistic, [Gaussian noise signals have been added to \$y\$](#) .

Since the observer (42) is local, the initial conditions of \hat{x} must be chosen sufficiently close to the actual initial condition $x(0) = 0$.

To test the robustness of this observer, several deviations on initial conditions and several noise measurements have been considered.

It is important to notice that, due to lemma 3, the characteristic damping of $\bar{e} = [e_1, e_2]^T$ is α . Moreover, the time constant of the observer is governed by α and χ . The arbitrary damping coefficient χ in $\hat{\mathbb{A}}$ can be preferentially chosen greater than the fixed constant α . In practice, it is natural to choose $\chi \approx \alpha$ (or slightly greater than α).

Figure 2 presents a quasi ideal situation with initial conditions close to the actual ones and low noise. It can be seen that the proposed observer has a pretty good behavior. More precisely, the observer \hat{x} converges rapidly towards x and [the measurement noise is weakened quite well](#).

In Fig. 3, initial conditions have been chosen quite far from the real ones: the error $(p^+(0) - \hat{p}^+(0))$ is about 20% of the mouth pressure p_m . The obtained results show that the transient behavior is longer than in Fig. 2 as expected, but the observer succeeds in retrieving the real value of the state.

Figure 4 shows that for larger measurement noises, the observer is still available ($\sigma_{noise}/p_m \approx 4\%$ seems to be closed to the limit, here).

Figure ?? illustrates the robustness with respect to deviations on parameters α , p_m and ω . After 0.15s, the error on initial conditions seems to be rejected and, despite the noise measurements and the deviation on parameters, the observer is locked on the original system dynamics. In particular, we can notice that even the behaviour of the lip states (x_1, x_2) is still relevant.

Finally, Fig. 6 shows that increasing χ improves the convergence: now the transient part only lasts about 0.6s and the estimation error is smaller than in Fig. 5. More generally, we have observed that: using $\chi \ll \alpha$ gives bad results (the observer converges too slowly); using the natural choice $\chi \approx \alpha$ (natural damping time scale of the original system) is satisfying; using larger values improves the observer convergence (but of course, too high values will also capture the noise).

Notice that since $y = (1 + \lambda)x_3$ is a “measured” quantity, in a simpler approach, it is not necessary to estimate x_3 and **it could have been sufficient to elaborate observer based on x_1 and x_2 only**. Nevertheless, since there are noise measurements, the total observer proposed here proves to be more robust. Indeed, in Figs. 2, 3, 4, the noise on \hat{x}_3 has been significantly reduced compared to that on y .

VI. CONCLUSION

In this paper, a nonlinear observer of a simplified model of a brass instrument (a lip blown cylinder with frequency independent losses) has been introduced. It has been proved using Lyapunov function techniques on neutral systems that the observer gains can be tuned to ensure the asymptotic stability of the linearized estimation error equation. Moreover, although the proof ensures only local stabilization, simulation results exhibit good robustness properties with respect to wrong initial conditions and significant noise on the measured output.

Future works could consist in improving both the resonator and the exciter models. For the resonator, models based on e.g. the Webster equation with realistic (frequency-dependent) losses [27, 28] could be considered. For such a model, associated Lyapunov functionals are available so that our approach could probably be adapted. For the exciter, the problem of finding sufficiently simple energy-balanced models is under study: their energy functional could constitute a Lyapunov functional candidate. Using the total energy of the instrument could help to derive a globally asymptotic observer.

Another work will concern the second problem (P2) described in the introduction, that is, computing the “player’s gestures” from the measured output and the proposed observer. It could be processed by using adaptive filtering techniques and would thus complete the global inversion problem.

Acknowledgments

The authors thank Silviu Niculescu for his helpful advices. This work has been supported by the CONSONNES project, ANR-05-BLAN-0097-01.

-
- [1] A. Chaigne and J. Kergomard. *Acoustique Des Instruments De Musique (The Physics of Musical Instruments)*. Belin, Paris, France, Echelles edition, 2008.
 - [2] N H. Fletcher and T. D. Rossing. *The Physics of Musical Instruments*. Springer-Verlag, New York, USA, 1998.
 - [3] Thomas Hélie, Christophe Vergez, Jean Lévine, and Xavier Rodet. Inversion of a physical model of a trumpet. In *Proc. of the Conference on Decision and Control*, volume 38.3, pages 2593–2598, Phoenix, Arizona, USA, 1999. IEEE.
 - [4] E. H. Wold. *Nonlinear parameter estimation of acoustic models*. PhD thesis, Computer Science Division, Berkeley University of California, USA, 1987.
 - [5] C. Vergez and X. Rodet. Bifurcation sequence in a physical model of trumpet-like instruments : From a fixed point to chaos. In *NOLTA*, volume 2, pages 751–754, Crans Montana, Switzerland, September 1998. IEICE.

- [6] T. Kailath. *Linear systems*. Prentice-Hall, Oxford, UK, 1980.
- [7] B. d'Andréa Novel and M. Cohen de Lara. *Commande linéaire des systèmes dynamiques (Linear control of dynamical systems)*. Modélisation Analyse Simulation Commande. Masson, Paris, France, 1994.
- [8] L. Ljung. *System Identification - Theory For the User*. Prentice Hall, Upper Saddle River, N.J. 07458, USA, 2nd edition edition, 1999.
- [9] E. Walter and L. Pronzato. *Identification of Parametric Models: From Experimental Data*. Communications and Control Engineering. Springer-Verlag, Berlin-Heidelberg, Germany, 1997.
- [10] L. Wu, C. Wang, and Q. Zeng. Observer-based sliding mode control for a class of uncertain nonlinear neutral delay systems. *Journal of the Franklin Institute*, 345(3):233–253, 2008.
- [11] C. Vergez. *Trompette et trompettiste: un système dynamique non linéaire à analyser, modéliser et simuler dans un contexte musical (Trumpet and trumpeter: a nonlinear dynamical system to analyze, to model and to simulate in a musical context)*. PhD thesis, Université de Paris 6, France, 2000.
- [12] Xavier Rodet. One and two mass model oscillations for voice and instruments. In *ICMC: International Computer Music Conference*, pages 207–214, Banff, Canada, September 1995.
- [13] Xavier Rodet and Christophe Vergez. Nonlinear dynamics in physical models : From basic models to true musical-instrument models. *Computer Music Journal*, 3(23), 1999.
- [14] W. J. Strong. Computer simulation of a trumpet. *J. Acoust. Soc. Amer.*, 87:S138, 1990.
- [15] S. Adachi and M.-A. Sato. Trumpet sound simulation using a two-dimensional lip vibration model. *J. Acoust. Soc. Am.*, 99(2):1200–1209, 1996.
- [16] C. Vergez and X. Rodet. Air flow related improvements for basic physical models of brass instruments. In *International Computer Music Conference*, Berlin, Germany, 2000. ICMC.
- [17] A. Hirschberg. *Mechanics of Musical Instruments, CISM Courses and Lectures*, volume 355, chapter chapter 7, pages 291–369. Springer, Wien, Austria, 1995.
- [18] J.-P. Dalmont, J. Gilbert, and S. Ollivier. Nonlinear characteristics of single-reed instruments: Quasistatic volume flow and reed opening measurements. *J. Acoust. Soc. Am.*, 114:2253–2262, 2003.
- [19] J. Hale and S.M. Verduyn Lunel. *Introduction to Functional Differential Equations*. Springer-Verlag, New York, USA, 1993.
- [20] W. Michiels and S.-I. Niculescu. *Stability and stabilization of time-delay systems. An*

- eigenvalue-based approach*, volume 12 of *Advances in design and control*. SIAM, Philadelphia, USA, 2007.
- [21] R.E. Kalman. A new approach to linear filtering and prediction problems. *Journal of Basic Engineering*, pages 35–45, 1960.
- [22] W.-B. Castelan and E.-F. Infante. A liapunov functional for a matrix neutral difference-differential equation with one delay. *Journal of Mathematical Analysis and Applications*, 71(1):105–130, 1979.
- [23] J.-M. Coron. On the null asymptotic stabilization of the two-dimensional incompressible euler equations in a simply connected domain. *SIAM Journal of Control and Optimization*, 37(6):1874–1896, 1999.
- [24] C.-Z. Xu and G. Sallet. Exponential stability and transfer functions of processes governed by symmetric hyperbolic systems. *Journal of Control Optimisation and Calculus of Variations (ESAIM)*, 7:421–442, 2002.
- [25] J.-M. Coron, G. Bastin, and B. d’Andréa Novel. Dissipative boundary conditions for one dimensional nonlinear hyperbolic systems. *SIAM Journal of Control and Optimization*, 47(3):1460–1498, 2008.
- [26] J.-M. Coron, B. d’Andréa Novel, and G. Bastin. A strict lyapunov function for boundary control of hyperbolic systems of conservation laws. *IEEE Transactions on Automatic Control*, 52(1):2–11, 2007.
- [27] Housseem Haddar, Thomas Hélie, and Denis Matignon. A webster-lokshin model for waves with viscothermal losses and impedance boundary conditions: strong solutions. In *Waves - International Conference on Mathematical and Numerical Aspects of Wave Propagation Phenomena (INRIA)*, volume 6, pages 66–71, Jyvaskyla, Finland, 2003.
- [28] Thomas Hélie. Mono-dimensional models of the acoustic propagation in axisymmetric waveguides. *J. Acoust. Soc. Amer.*, 114:2633–2647, 2003.

Tables

Table I: Reduced parameters (σ denotes $\sigma = \text{sign}(\xi)$).

σ	α	ω	β_0	β_m
+	$\frac{a}{m}$	$\sqrt{\frac{k}{m}}$	$\frac{A_{bot} - A_{side} \sin \theta}{m}$	$\frac{A_{side} \sin \theta}{m}$
-	$\frac{1+\kappa_a}{1+\kappa_m} \alpha^+$	$\sqrt{\frac{1+\kappa_k}{1+\kappa_m}} \omega^+$	$-\frac{A_{side} \sin \theta}{(1+\kappa_m)m}$	$\frac{A_{side} \sin \theta}{(1+\kappa_m)m}$
$\tau = 2L/c$		$\lambda = (Z_L - Z_c)/(Z_L + Z_c)$		$\mu = S^2/(\rho \ell^2 c^2)$

Figures

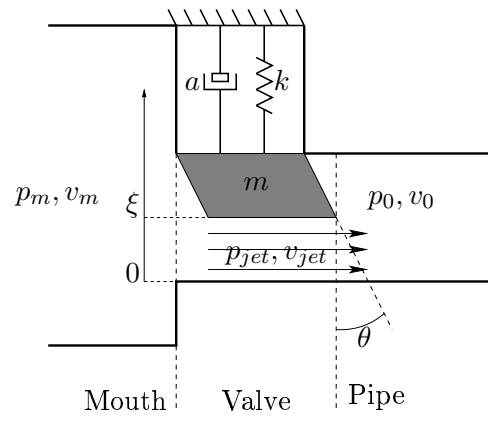


Figure 1: The dynamics of the musician's lips are modeled by that of a solid mass subjected to pressure forces, a damper and a spring. Variables p denote (relative) pressures and variables v denote particle velocities.

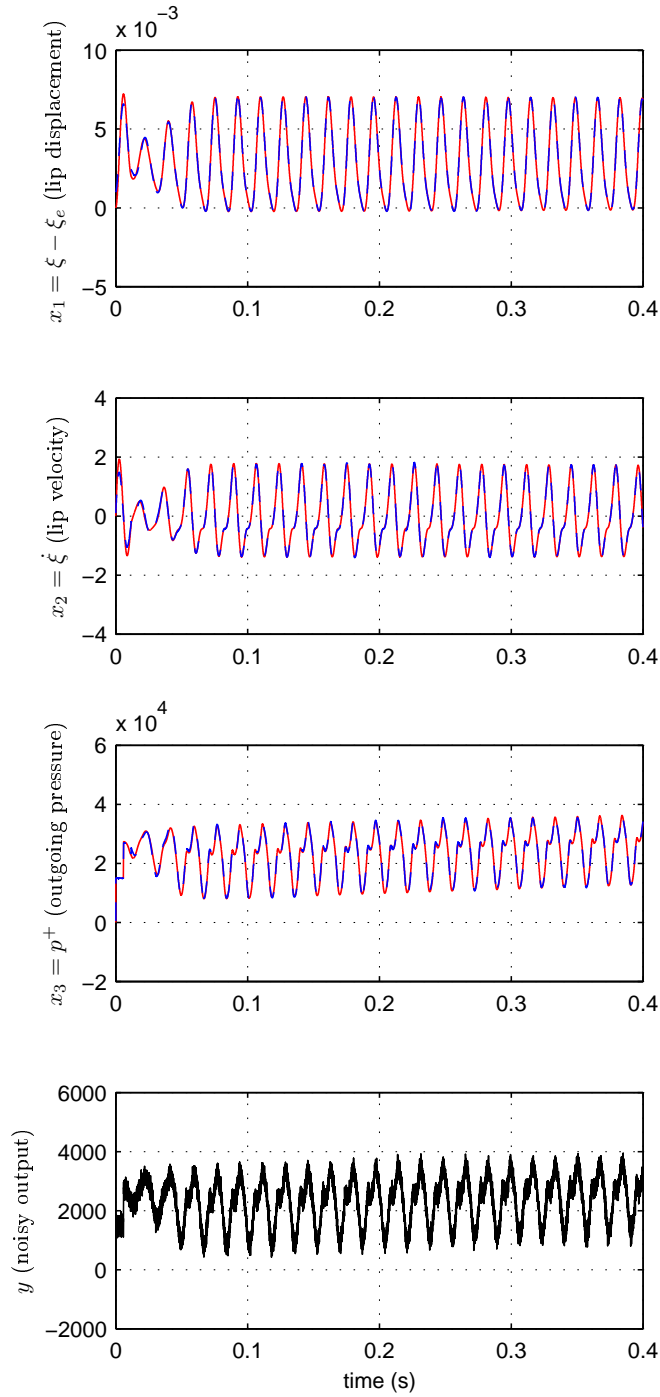


Figure 2: Simulation of the system (-) and of the observer (- -) from the noisy output y (-). The simulations are performed for the following parameters: $\alpha = 150s^{-1}$, $\chi = 160s^{-1}$, $L = 1$, $p_m = 1.5e4Pa$, $\omega = 535s^{-1}$, quasi-ideal initial conditions $\hat{x}(0) = [1e - 3, 1e - 1, \frac{y(0)}{1+\lambda}]^T$ and low noise $\sigma_{noise}/p_m = 0.01$.

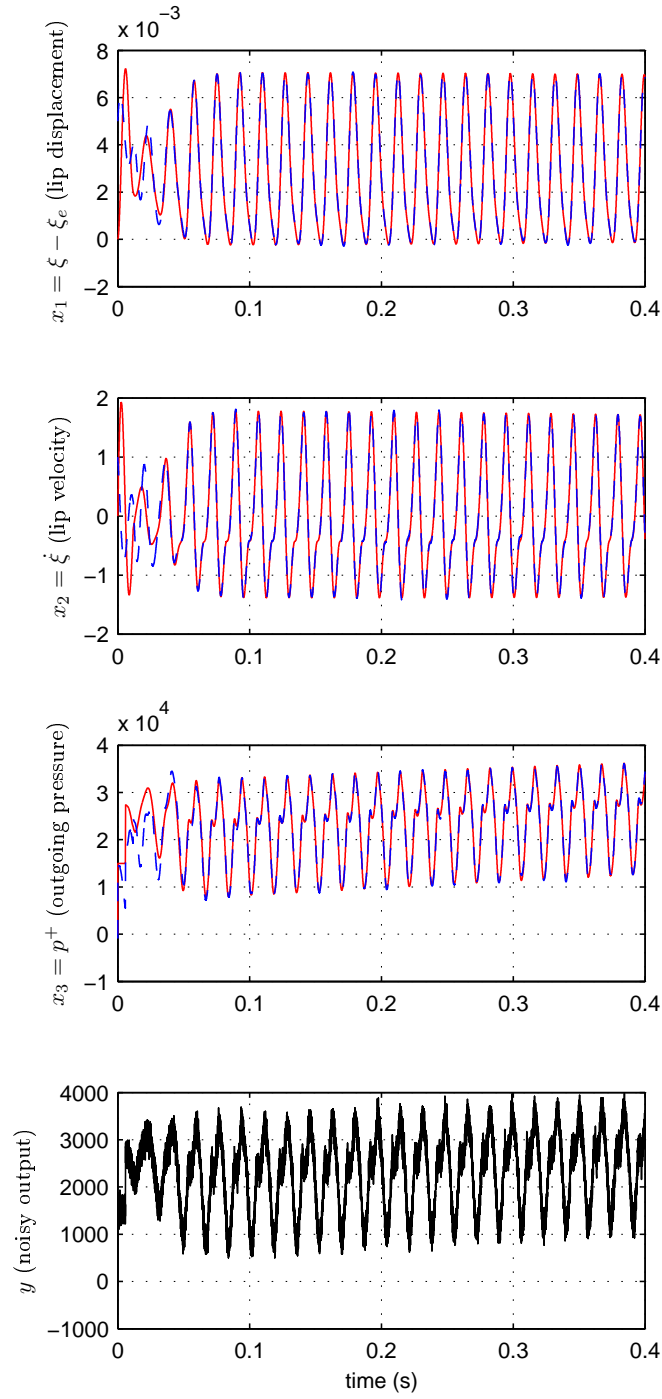


Figure 3: Simulation of the system (-) and of the observer (- -) from the noisy output y (-). The simulations are performed for the following parameters: $\alpha = 150s^{-1}$, $\chi = 160s^{-1}$, $L = 1$, $p_m = 1.5e4Pa$, $\omega = 535s^{-1}$, a large deviation on initial conditions $\hat{x}(0) = [5e - 3, 1, \frac{y(0)}{1+\lambda}]^T$ and low noise $\sigma_{noise}/p_m = 0.01$.

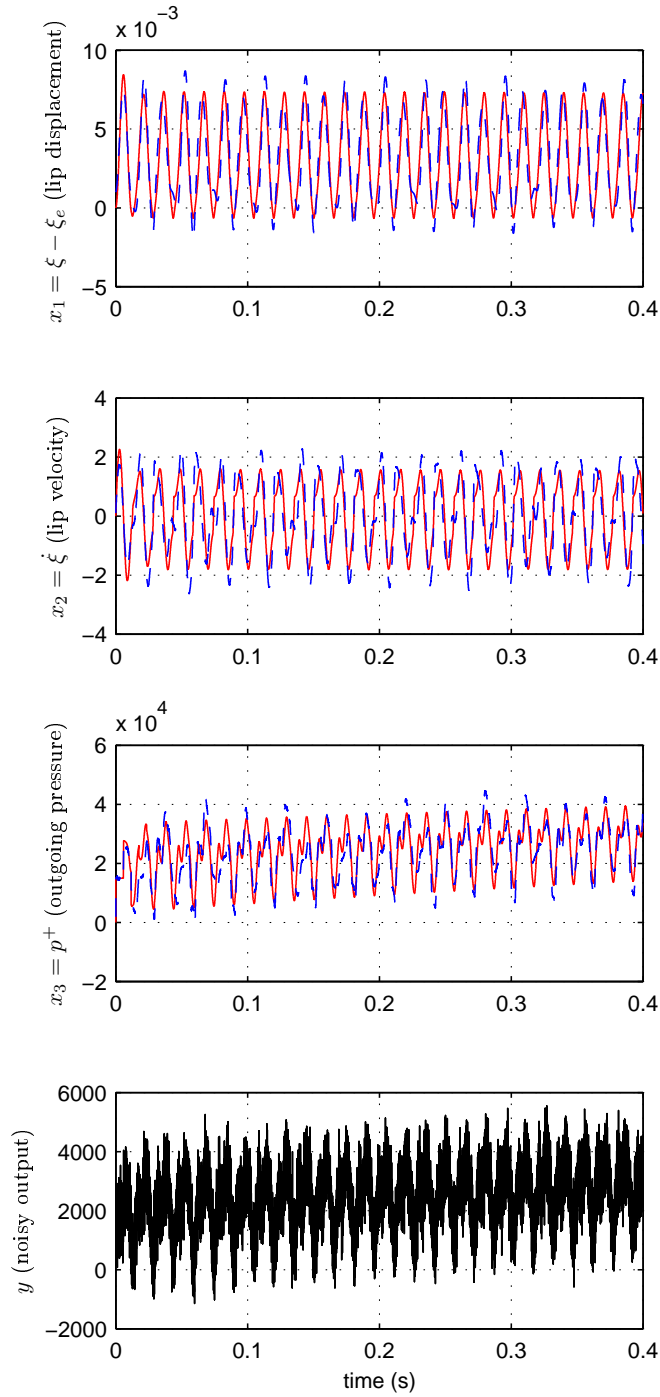


Figure 4: Simulation of the system (-) and of the observer (- -) from the noisy output y (-). The simulations are performed for the following parameters: $\alpha = 150s^{-1}$, $\chi = 160s^{-1}$, $L = 1$, $p_m = 1.5e4Pa$, $\omega = 535s^{-1}$, quasi-ideal initial conditions $\hat{x}(0) = [1e-3, 1e-1, \frac{y(0)}{1+\chi}]^T$ and large noise $\sigma_{noise}/p_m = 4e-2$.

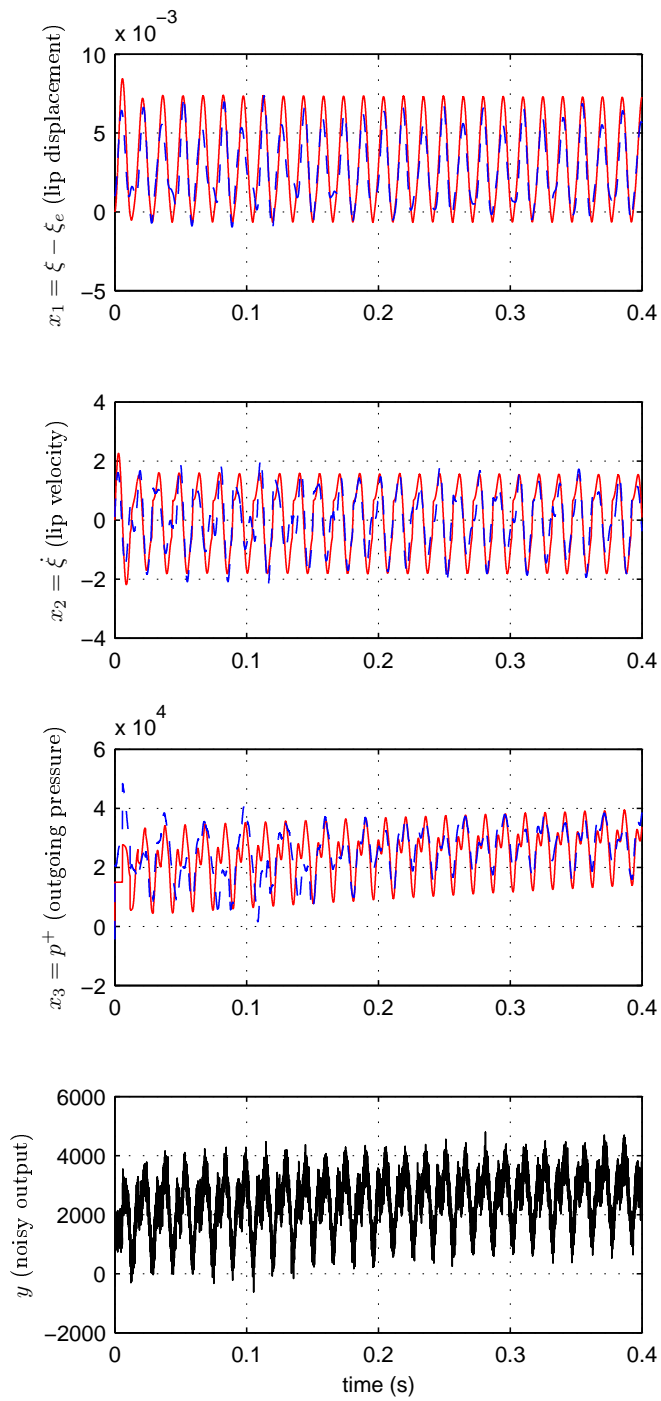


Figure 5: Simulation of the system (-) and of the observer (- -) from the noisy output y (-) and with parameters deviations. For the original system, simulations are performed with the following parameters: $\alpha = 150s^{-1}$, $\chi = 160s^{-1}$, $L = 1$, $p_m = 1.5e4Pa$, $\omega = 535s^{-1}$. The added noise corresponds to $\sigma_{noise}/p_m = 0.02$. For the observer, simulations are performed with the following wrong parameters: $\alpha^o = 1.1\alpha$, $p_m^o = 1.1p_m$, $\omega = 1.1\omega^o$ and quasi-ideal initial conditions $\hat{x}(0) = [1e - 3, 1e - 1, \frac{y(0)}{1+\lambda}]^T$.

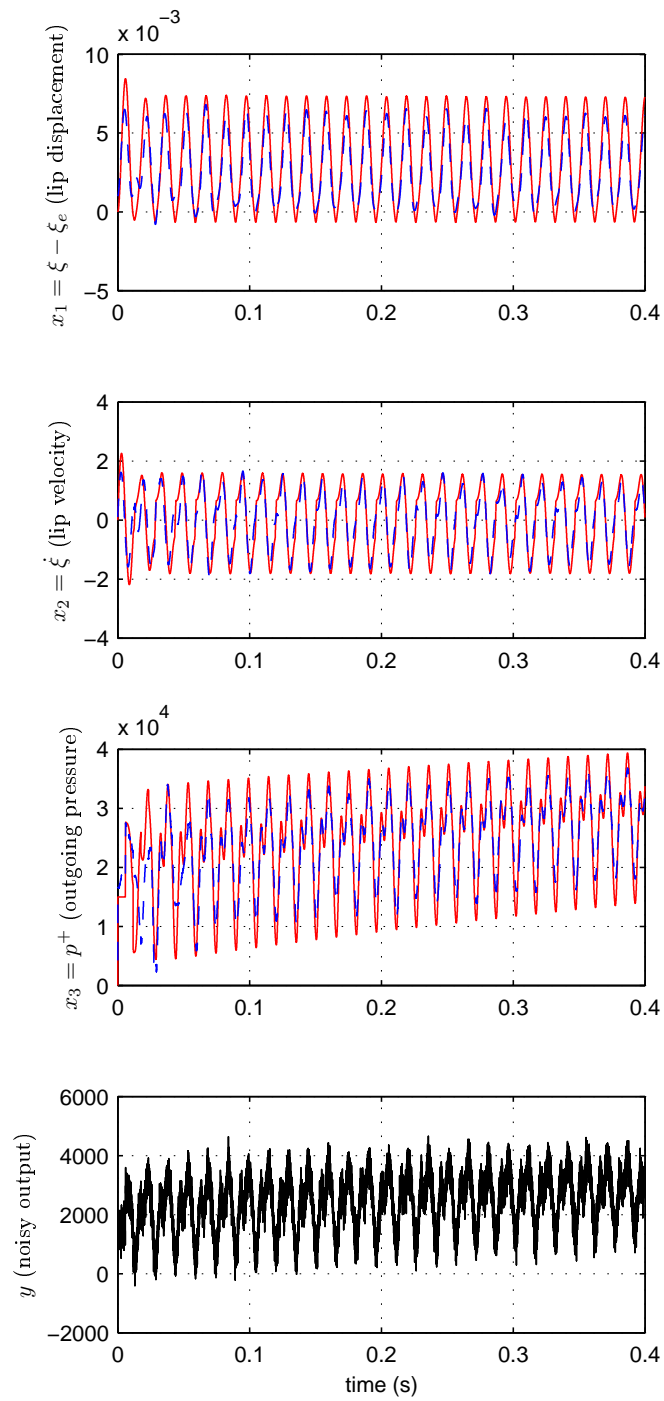


Figure 6: Idem than Fig. 5 but with $\chi = 2 \times 160s^{-1}$.